Laser-Sustained Plasmas in Forced Argon Convective Flow, Part I: Experimental Studies

Richard Welle,* Dennis Keefer,† and Carroll Peters‡
University of Tennessee Space Institute, Tullahoma, Tennessee

The results of an experimental investigation of the properties of laser-sustained plasmas in argon at forced convective flow speeds of 0.4–4.5 m/s are reported in this paper. At these speeds, the incident flow rate has a significant effect on the shape, size, and position of the plasma, which in turn affect the power absorption, thermal radiation, and total energy conversion efficiency of the plasma. In addition to the incident flow rate, the focusing geometry, chamber pressure, and laser power were varied as parameters in the experiments. The thermal conversion efficiency was found to range 9–38%, depending on the various parameters.

Introduction

SEVERAL laser thermal propulsion concepts[1-4] were proposed during the 1970's and the laser-sustained plasma (LSP) was recognized as an effective means to absorb laser power into a propellant in the steady-state mode. A collimated laser beam from a remote site is focused into an absorption chamber, which is analogous to the combustion chamber in a conventional chemical rocket. Laser power is absorbed by and sustains a high-temperature plasma core (about 15,000–20,000 K), which mixes with the cold buffer flow of propellant downstream, heating the flow to the maximum temperature that the chamber wall material can tolerate. Then the flow is accelerated through a conventional nozzle to produce the required thrust. The major advantages of laser thermal propulsion compared to chemical propulsion are that the propellant having the lowest molecular weight (pure hydrogen) can be used and that the maximum temperature of the working fluid is not limited to the flame temperature of a combustion process. An estimated specific impulse for laser thermal propulsion using hydrogen propellant[5] is in the range of 1000–1500 s, which is about three times that of the most advanced chemical propulsion system. The relative high specific impulse, along with the thrust levels that can be achieved (roughly 100 N/MW of incident laser power), makes this laser propulsion concept attractive for orbital transfer missions.

The LSP used for power absorption would have to be stable in a forced convective flow and to absorb nearly all energy in the incident laser beam. In an effort to understand the relevant physics, our group has undertaken a series of experimental and analytical studies of the effect of a forced convective flow on the characteristics of the LSP in argon.

Previous experimental investigations of laser-sustained plasmas have been conducted in buoyancy-dominated flows, either with no flow controls[6-8] or with a forced convective flow limited to speeds on the order of those generated by buoyancy effects ($\approx$30 cm/s).[9-11] The effect of forced convective flow in this speed range has proven to be negligible and the energy conversion efficiency of the LSP has been determined by the other principle variables: ambient pressure, incident laser power, and focusing geometry. In this paper, we are reporting for the first time the results of measurements made on argon plasmas sustained in a forced convective flow at flow speeds significantly above those generated by buoyancy effects. Laser-sustained plasmas are also being investigated theoretically and the current status of these investigations is discussed by Jeng et al. in an accompanying paper.[12]

Experimental Procedure

The plasmas sustained in these experiments were contained in a 22 mm i.d. cylindrical quartz flow tube with a converging entrance section. A diagram of the experimental apparatus is shown in Fig. 1. The laser power was provided by an axial-flow, electric discharge, carbon dioxide laser that provides a nominal 1 kW continuous beam. The beam has an annular profile produced by an unstable oscillator of 1.5 magnification. The beam, $\approx$54 mm in diameter with good axial symmetry, was focused collinearly with the axis of symmetry of the flow tube. The apparatus was oriented with its symmetry axis in the vertical direction, with the laser beam propagating vertically upward to eliminate nonaxisymmetric buoyancy effects. This configuration generally provided for a plasma with good axial symmetry, which is required for accurate diagnostics.

The primary measurements acquired from the experiments were digital images of the plasma. These images were obtained by a CID video camera whose spectral range was limited by a narrow bandpass interference filter. The filter was chosen to isolate a 1 nm wide region of the continuum radiation from the plasma, free of line radiation and centered at 626.5 nm. The digital images were acquired using a digital image processing computer, which allowed images to be acquired at video frame rates (30/s) and averaged into memory. The entire image acquisition system was calibrated through the direct substitution of a standard lamp of spectral radiance.

In order to determine the fraction of the incident laser beam absorbed by the plasma, the position of the plasma relative to the focal zone of the beam must be known. This was achieved by mounting an acrylic block in the field of view of the camera such that the axis of symmetry of the laser beam would lie approximately in the plane of the surface of the block. The beam was then turned on in short, high-power bursts until all of the acrylic intercepting the beam was burned away. A digital image of this burn pattern was then acquired to determine the position of the laser focus relative to the field of view of the camera. The uncer-

Presented as Paper 86-1077 at the AIAA/ASME Fourth Fluid Mechanics, Plasma Dynamics and Lasers Conference, Atlanta, GA, May 12–14, 1986; received May 21, 1986; revision received Jan. 21, 1987.

*Predoctoral Fellow, Center for Laser Applications (presently, Member, Technical Staff, The Aerospace Corporation, El Segundo, CA). Student Member AIAA.

†Professor, Engineering Science and Mechanics, Center for Laser Applications. Member AIAA.

‡Professor, Mechanical and Aerospace Engineering, Center for Laser Applications. Member AIAA.

tainty in the location of the circle of least confusion, as measured by this method, was approximately ±15 pixels, or about ±½ mm. Knowing this uncertainty is important in determining the precision of the power absorption calculations.

In contrast to earlier experiments, the high incident flow rates used in the current set of experiments resulted in plasmas whose position relative to the focal zone of the laser beam could be controlled by the flow. In order to keep the plasma within the flow tube and within the field of view of the camera, the sodium chloride focusing lens was mounted on a calibrated vertical-axis translation stage and was moved as necessary during the experiments to position the plasma within the field of view of the camera. Additional details of the apparatus and experimental procedure have been described in earlier papers.[10,11]

Data Analysis

The eight-bit digital images of the plasma contained 240×512 pixels obtained from single-field scans of the camera. In each case, 16 sequential images were averaged in memory to improve the signal-to-noise ratio in the low-intensity regions of the plasma. In a typical plasma image, the plasma is 7 mm in diameter and 10 mm long, covering 130 pixels in the radial direction and 320 pixels in the axial direction. The camera background was subtracted from this image and an Abel inversion of the resulting image was performed using Fourier techniques that will be described in a later paper. (These methods were compared with the Abel inversion technique described in our earlier work[10,11] and were found to produce identical results without requiring subsampling and at a substantial savings in computer time.) By applying the appropriate calibration factors, the emission coefficient was obtained as a function of position in the plasma and, from this, the temperature was obtained by interpolation in tabulated data published by Morris.[13]

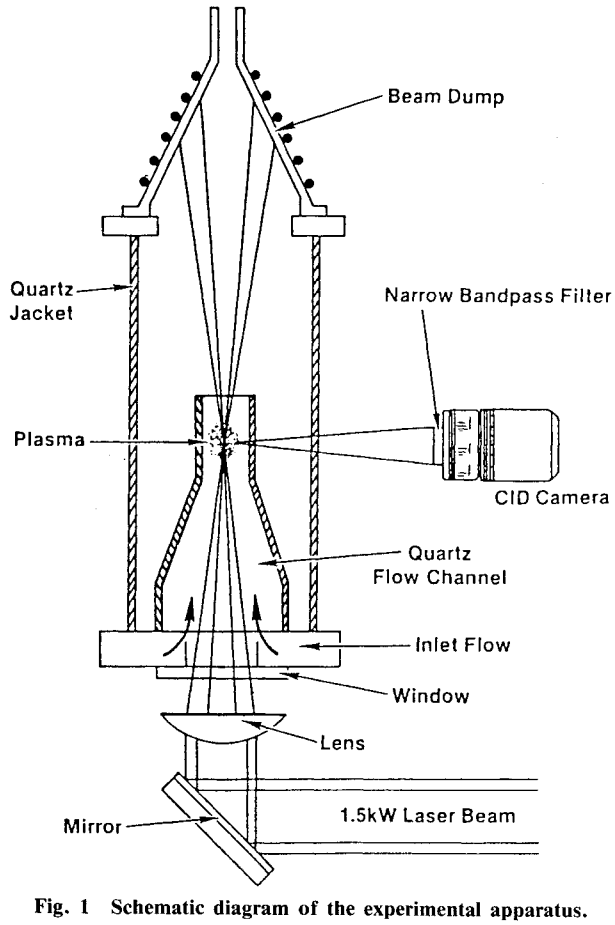

Fig. 1 Schematic diagram of the experimental apparatus.

The thermal radiation loss in the plasma was determined using the relation published by Kozlov et al. for optically thin radiation,[14] and the absorption coefficient at 10.6 μm was calculated according to the method described by Kemp and Lewis[15] using the thermodynamic data tabulated by Drellishak et al.[16] and the Gaunt factors published by Karzas and Latter.[17] To calculate the total power absorption, the measured annular profile of the incoming laser beam was broken into discrete rays, each representing a fraction of the incident radiation. Each ray was traced, using geometric optics, through the sodium chloride focusing lens and window and then through a grid system superimposed on the measured temperature field of the plasma. At each step through the grid, the power absorbed from each ray was subtracted from the ray and added to the plasma. This procedure gave both the spatial distribution of power absorption and the total power absorbed by the plasma. Subtracting the thermal radiation loss from the total power absorbed gave the total energy conversion efficiency of the plasma.

In previous work, the refraction of the rays by the inhomogeneous index of refraction in the plasma was neglected. This effect has now been included in the analysis by calculating the index of refraction at each point in the grid system according to the relation published by Cheng and Casperson.[18] At each step of a ray through the grid system, a refraction gradient was approximated by the first-order radial difference of the refractive index. It was assumed that the axial component of the gradient could be neglected, as the ray was always within 9 deg of the axis and it was only the normal component of the refraction gradient that caused deflection of the ray. The angle of deflection of a ray in any grid cell was proportional to the product of the gradient and the path length in the cell. The refraction of the ray was then effected in the power absorption calculations by adding this calculated deflection angle to the propagation path of the ray before going on to the next cell.

To evaluate the influence of refraction on the absorption efficiency, the ray trace was performed with the index of refraction defined uniformly over the plasma with a value of 1.0 and the results were compared with the results obtained using the calculated inhomogeneous index of refraction. In our earlier work, this effect appeared to cause a change in the calculated power absorption of up to 5%, but with the present set of data, there was no variation in excess of 1%. The difference is most likely due to the greater uncertainty in the position of the plasma relative to the laser focus in the earlier work. An uncertainty in the axial position of the plasma will generate uncertainty in the power absorption in two ways: 1) if the plasma is offset a sufficient amount, the incident beam will not pass through the highest temperature portion of the plasma, resulting in an apparent reduction in the power absorption; and 2) as will be noted herein, in the current set of data the plasma is usually shaped such that the path of the beam at the leading edge of the plasma is normal to the temperature isotherms, minimizing the refraction effect on entry into the plasma. If the plasma is offset in the axial direction, the ray trace is more likely to enter the plasma on a path with a component parallel to the isotherms, resulting in an erroneously large calculated refraction effect at the leading edge, where any errors will propagate through the entire plasma. The uncertainty in the power absorption calculation resulting from these two effects was evaluated by introducing an offset into the plasma position and performing the calculations for several different plasmas. In no case did an offset of ½ mm in either direction result in a change of more than 2% in the fractional power absorption, but in certain cases, offsets of 2 mm resulted in 5+% changes in the fractional power absorption, with one case resulting in an 11% change at 2 mm offset.

In addition to the refraction of the beam in the plasma, there is also the effect of diffraction caused by the finite size of the lens aperture. This effect has been neglected in the

current study as it presents a much more difficult problem than refraction. A preliminary analysis indicated that the diffraction limited spot size is approximately twice the size of the spot calculated according to the geometric ray assumption. This effect would place a larger share of the incident energy away from the center axis and would likely result in a slight reduction in the total power absorption. Additional details of the data analysis procedure were described in an earlier paper.[11]

Experimental Results

The objective of these experiments was to investigate the effect of high incident flow rates on the behavior of laser-sustained plasmas and, specifically, the effect on energy conversion efficiency. At low incident flow rates ($\leq$30 cm/s), the position and shape of the plasma relative to the incident laser beam geometry was essentially unaffected by the flow. The plasma stabilized in the region of the focused beam, where the incident intensity was just sufficient to balance the thermal radiation, conduction, and convection losses from the plasma. In general, this means that the plasma stabilizes at a position upstream of the focus of the incident beam; this position depends on the incident power, focusing geometry, and ambient pressure. The plasma tends to fill the beam at the position of stabilization and therefore grows larger in diameter as it moves up the beam. When the incident flow rate is increased significantly beyond 30 cm/s, the flow tends to force the plasma to stabilize at a position further down the beam and closer to the focus. The plasma again tends to fill the beam, but because the beam is narrower near the focus, the plasma is smaller in diameter and lies in a region of greater laser intensity.

Figure 2 shows an isothermal contour plot for the high-temperature region of two plasmas sustained under similar conditions of pressure and laser power, but with substantially differing incident flow speeds. In these and all subsequent diagrams, the contour interval is 500 K with the outer isotherm at 10,500 K and the focal point of the laser (defined as the location of the circle of least confusion) is at the location labeled 50 mm on the x axis. In all cases, the flow is from left to right and the laser beam is incident from the left. With the low-flow case, the major portion of the plasma is upstream of the laser focus and there is a significant off-axis temperature peak. The temperature peak in this case occurs near the annular focus of the beam produced by spherical aberrations, as discussed in our earlier paper.[11] By comparison, the high-flow plasma stabilized with a significant fraction downstream of the focus, and has no significant off-axis temperature peak. In addition, the peak temperature of the high-flow plasma is much higher than that of the low-flow case: 15,500 K compared to 13,700 K.

The path of the incident laser beam through the plasma is also illustrated in Fig. 2 and in subsequent isothermal contour plots. The lines represent the approximate boundaries of the annular beam in an unrefracted path through the plasma. As was noted earlier, the incident beam in most cases enters the plasma on a path that is nearly perpendicular to the isotherms, which results in very little refraction of the beam before it passes through the high-temperature region of the plasma; the effect of refraction on power absorption is therefore minimized.

In Fig. 2, the path length of the beam through the two plasmas is about the same, but in the high-flow case the path has, on the average, a higher temperature, particularly in the region of highest laser intensity near the focus. This results in a significantly higher overall absorption efficiency: 83% compared to 66%. At the same time, because the overall size of the high-flow plasma is smaller than the low-flow plasma and, because the highest-temperature region is confined to a very small volume near the axis, the overall thermal radia-

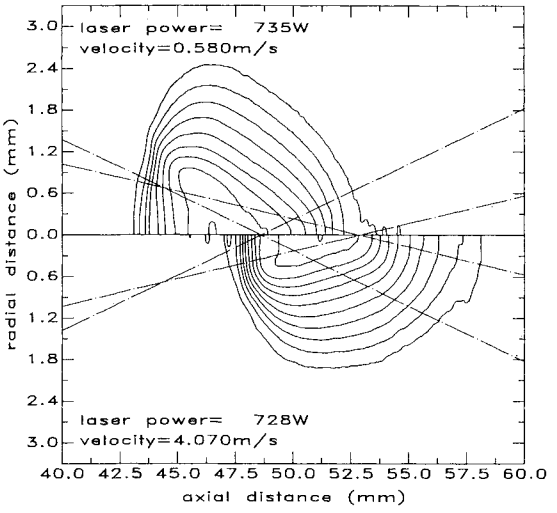

Fig. 3 Isothermal contour plots of two plasmas sustained using the 8 in. lens at 2.5 atm pressure. The contour interval is 500 K, with the outer contour at 10,500 K.

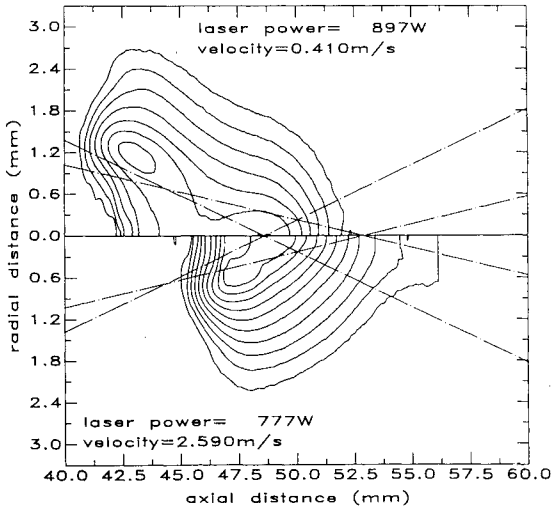

Fig. 2 Isothermal contour plots of two plasmas sustained using the 8 in. lens and a chamber pressure of 3 atm. The contour interval is 500 K, with the outer contour at 10,500 K.

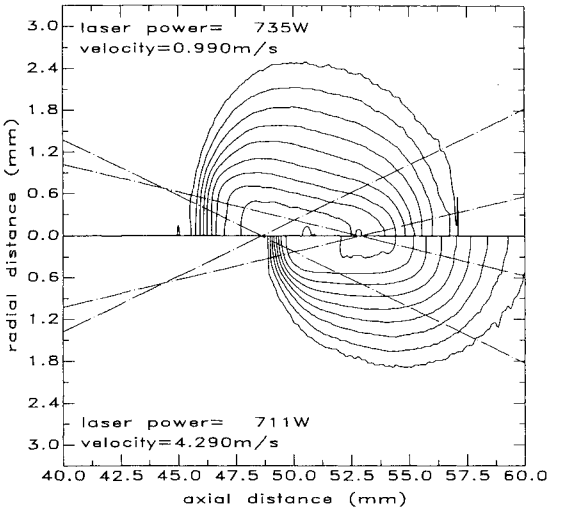

Fig. 4 Isothermal contour plots of two plasmas sustained at 1.5 atm with the 8 in. lens. The contour interval is 500 K, with the outer contour at 10,500 K.

tion loss increased by only 3%, from 54 to 57% of the incident radiation. The energy conversion efficiency, from laser to thermal energy in the flow, increased from 12 to 26% as a result of the increase in the flow.

When the chamber pressure is reduced, similar results are obtained. Figure 3 shows the effect at 2.5 atm; note the reduced tendency toward an off-axis temperature peak as the absorption coefficient decreases with the pressure. The increase in flow in this case has the effect of making the plasma relatively longer and narrower and reducing the diameter of the 10,500 K contour by 1 mm, while increasing the length by about the same amount. The value of the peak temperature increased from 14,600 to 15,600 K with the increase in flow, but the highest-temperature region was again confined to a very small volume in the focal zone of the incident beam. This resulted in an increase of absorption efficiency from 67 to 78%, while the thermal radiation loss was actually reduced from 53 to 45% of the incident radiation. The net energy conversion efficiency increased from 14 to 32% as a result of the increase in flow.

It is worth noting that the maximum incident flow rates investigated in this series of experiments were limited in the low-pressure experiments by the capacity of the flow system and in the high-pressure cases by the capacity of the available flow meter. In no case was there any indication of plasma instability caused by high flow rates. The only noticeable unsteadiness occurred in high-pressure, low-flow plasmas, but none was spontaneously extinguished. The minimum flow rate in all cases was limited to the minimum mass flow that would register on the meter.

At 1.5 atm, Fig. 4 shows the effect of flow speeds somewhat higher than those available at higher pressures. In the low-flow case, the plasma was centered very near the focus of the incident laser beam and was relatively symmetric along the axis, with the temperature gradient on the upstream boundary about double that at the downstream boundary. When the flow speed was increased by a factor of four, the plasma moved downstream to where the 10,500 K contour on the leading edge was only 1 mm upstream of the focus, with a very strong temperature gradient, while the trailing edge was roughly 10 mm downstream of the focus, with a very weak temperature gradient. In this case, the higher flow rate pushed a sufficient portion of the plasma beyond the high-intensity region to cause a reduction in the absorption efficiency of the plasma from 56 to 44%. The smaller size of the plasma also caused a reduction in the thermal radiation loss from 38 to 23% of the incident laser power. The combined effects result in only a very small change in the energy conversion efficiency of the plasma, increasing it from 18 to 21% with the increase in flow speed.

Figures 2–4 represent the endpoints of three series of plasmas. The data for the intermediate values of flow are shown in the next three figures. In Fig. 5, at 1.5 atm, the trend with increasing flow is a monotonic decrease in both power absorption and thermal radiation loss. The difference between the two represents the total energy conversion efficiency, which shows a weak maximum near 350 cm/s, but the magnitude of the peak is probably smaller than the uncertainty in the calculations.

At 2.5 atm (Fig. 6), the absorption efficiency shows a peak near 300 cm/s, while the thermal radiation loss peaks near 100 cm/s. The conversion efficiency increases with the flow until about 300 cm/s, after which it is nearly constant at 30%. At 3 atm (Fig. 7), the thermal radiation loss appears to peak around 200 cm/s, while the absorption efficiency does not reach a peak in the range of flow speeds observed. The maximum conversion efficiency for this pressure level, therefore, occurs at a flow rate somewhere above 250 cm/s. (It should be noted that we had some difficulty holding the laser power constant in this series, with a variation between 900 W for the low-flow case and 780 W for the high-flow case, which is a possible cause for the apparently anomalous behavior of the absorption and thermal reradiation curves at 41 cm/s. In the two lower-pressure series, the laser power was held within the range of 705–735 W. The effect of laser power changes will be discussed below.)

Some indications of the effects of chamber pressure are seen in the three sets of isothermal contour plots (Figs. 2–4).

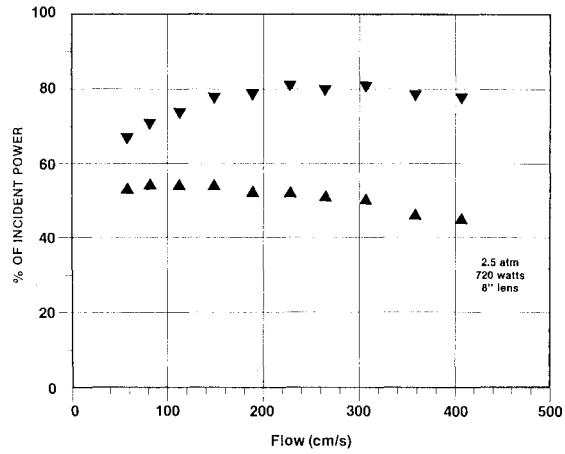

Fig. 6 Graph of variation in power absorption ▽ and thermal radiation loss △ with flow rate for a series of plasmas sustained at 2.5 atm.

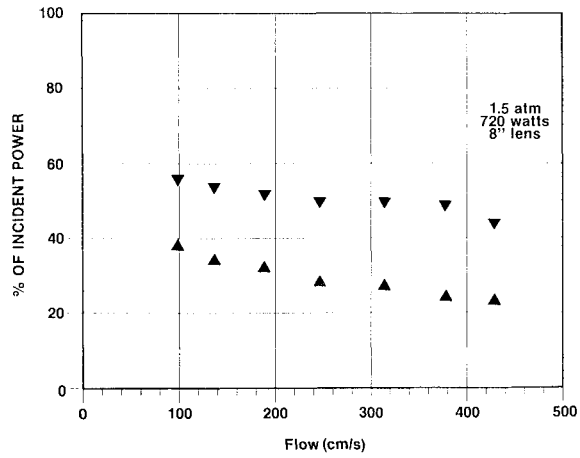

Fig. 5 Graph of variation in power absorption ▽ and thermal radiation loss △ with flow rate for a series of plasmas sustained at 1.5 atm.

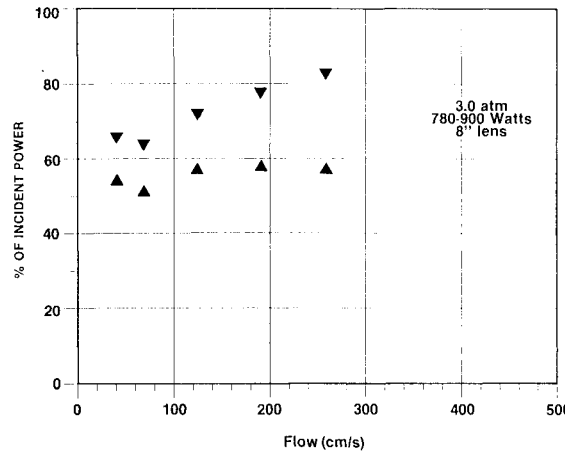

Fig. 7 Graph of variation in power absorption ▽ and thermal radiation loss △ with changing flow rate for a series of plasmas sustained at 3 atm.

At high pressures, the absorption coefficient is sufficiently high to allow the plasma to move upstream into a region of lower laser intensity. With the annular laser beam this can, in extreme cases, result in large-diameter plasmas with off-axis temperature peaks. Because of the lower laser intensity in the annular focus relative to the axial focus, the magnitude of a typical off-axis temperature peak is lower than that of one on the axis, resulting in lower power absorption efficiency. At the same time, the large plasma diameter ensures that the thermal radiation loss remains large. The effects are illustrated in Fig. 8, where the power absorption and thermal radiation losses are shown as functions of pressure for a given mass flow rate. (It must be emphasized here that this series is at a constant mass flow rate, so the incident flow speed is an inverse function of the chamber pressure.) At the lowest pressures, the flow speed is high enough to force most of the plasma downstream of the focus, so that the plasma resembles the high-flow case of Fig. 4 and the absorption and thermal radiation losses are correspondingly low. As the pressure increases and the flow speed decreases, the plasma moves upstream. At 2 atm, it is approximately centered on the focal volume and, at 4 atm, it has moved so far upstream that there is essentially no plasma at the axial focus. The net result is that both the absorption and the total energy conversion efficiency go through a peak at just above 2 atm pressure, when the plasma is just slightly upstream of the focus. Although this was the only pressure series we ran, the graphs of Figs. 5-7 indicate that at higher flow rates, this peak may occur at higher pressures.

The influence of the focusing geometry on the plasma stability and energy conversion efficiency was also modified by higher incident flow rates. In an earlier paper,[11] we reported that we were unable to initiate or sustain a plasma at pressures greater than 2 atm using a 12 in. focal length lens (f/5.6 with a beam diameter of 54 mm). The incident flow speed in that set of experiments was limited to less than 15 cm/s. As the pressure increased, at a constant mass flow rate, the plasma would move upstream until, at 2 atm, it became unstable. At much higher flow speeds, however, we had no trouble initiating and sustaining plasmas with the 12-in. lens at pressures up to 3 atm. Figure 9 shows a pair of isothermal contour plots of 2.5 atm plasmas that illustrate this effect. The axial scale has again been selected such that the focal point of the laser is at the value 50 mm. In the low-flow case, the leading edge of the plasma has moved upstream to a point 10 mm ahead of the focus and there is no plasma at the focal point. The peak temperature in this plasma is 14,200 K and the highest-temperature region is mostly located away from the axis, giving it a relatively large volume. The net result is a very poor energy conversion efficiency of only 12%. In the high-flow case, the plasma has been forced into a location approximately centered on the focal zone, with the diameter at all temperature contours decreased by about 1 mm and the overall length increased by about 3 mm. The peak temperature has increased to 16,300 K, and the highest temperature zone is confined to a narrow cylinder along the axis. These effects combine to provide an energy conversion efficiency of 38%, the highest observed in any of our current series of plasmas.

A comparison between the results of this flow series using the 12 in. lens (f/5.6) and a similar series using the 8 in. lens (f/3.8), both at 2.5 atm, is shown in Fig. 10. The conversion efficiency in the f/5.6 series is clearly tending toward zero as the flow is decreased, indicating that the plasma will become unstable in this flow region. As mentioned, this instability was observed in previous experiments. It is also seen that the flow rate at which the peak efficiency occurs increases with the increase in focal length. Further insight into this effect can be obtained by comparing the high-flow cases at two different f/numbers as shown in Fig. 11; both cases are 2.5 atm plasmas sustained at approximately 720 W and a 4 m/s flow rate. The f/3.8 plasma is centered about 2 mm downstream of the focus and has a peak temperature of 15,600 K, while the f/5.6 plasma is centered within ½ mm of the focal point,

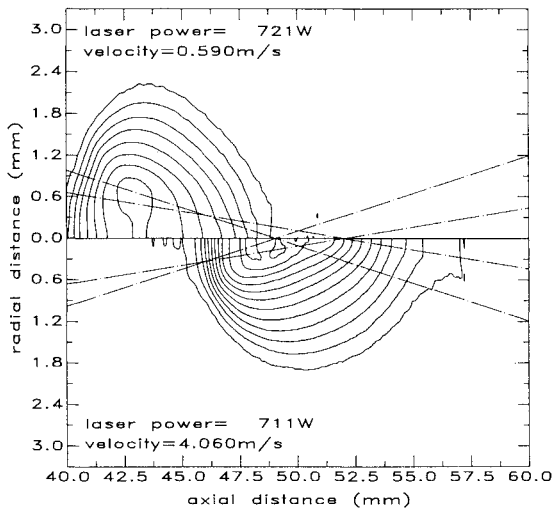

Fig. 9 Isothermal contour plots of two plasmas sustained at 2.5 atm using the 12 in. focal-length lens. The contour interval is 500 K, with the outer contour at 10,500 K.

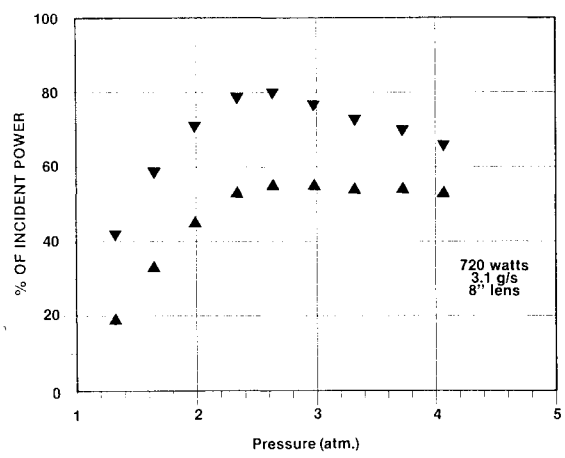

Fig. 8 Graph of variation in power absorption ▽ and thermal radiation loss Δ with pressure for a series of plasmas sustained at a constant mass flow rate.

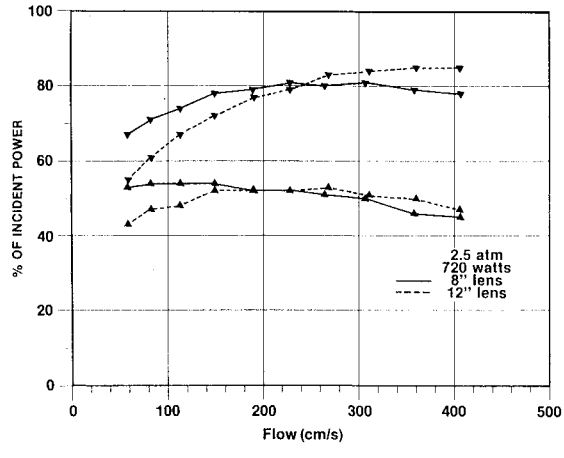

Fig. 10 Graph showing the effect of flow rate on power absorption ▽ and thermal radiation loss Δ for plasmas sustained at 2.5 atm using two different focal length lenses.

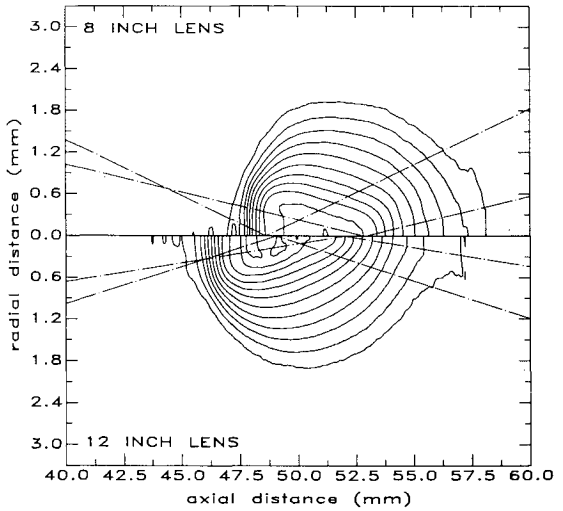

Fig. 11 Isothermal contour plots of two plasmas sustained at 2.5 atm in a 4 m/s incident flow, with 720 W incident power and using two different focusing lenses. The contour interval is 500 K, with the outer contour at 10,500 K.

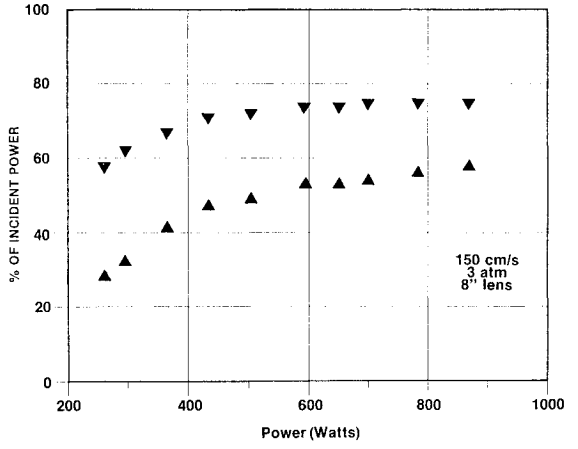

Fig. 12 Graph of variation in power absorption ▽ and thermal radiation loss Δ with changing incident power level. The plasmas in this series were sustained with the 8 in. lens at 3.0 atm and 160 cm/s flow speed.

is just slightly smaller in diameter, and has a peak temperature of 16,200 K. Because of the narrower angle of convergence of the beam, the flow speed required to force the plasma into the downstream region of the focal zone, where the efficiency begins to deteriorate, is higher for the larger f/number lens. This indicates the possibility of sustaining stable plasmas with very long focal length lenses, provided the forced convective flow is sufficiently fast.

We turn now to the effect of changing laser power. Figure 12 is a typical graph of the variation in the power absorption and thermal radiation loss with changing laser power in a series of plasmas where the pressure and flow rate were held constant. On the low-power end, as expected, the absorption begins to fall off rapidly as the minimum maintenance threshold is approached. As the power is increased, the absorbed fraction increases asymptotically to 75%, with no indication of a trend toward a subsequent decrease. In two other series (not shown), a similar effect was observed, with the asymptote being a function of the pressure, flow rate, and focusing geometry. In a fourth series, sustained at 1.5 atm and 315 cm/s with the 12 in. lens, the absorbed fraction continued to increase at the maximum available laser power, reaching 67% at 932 W incident power.

In Fig. 12, we see also that the thermal radiation loss fraction continues to increase with increasing power and with no apparent asymptote, although it obviously cannot exceed the absorbed fraction. This effect was observed in each of the power series. In the series of Fig. 12, the total energy conversion efficiency appears to be decreasing slightly with increasing flow. The other three power series were sustained with the 12 in. lens, all at approximately the same mass flow rate but at different pressures and hence different flow speeds. At 3 atm and 150 cm/s, the total conversion efficiency appeared to decrease with increasing power, as in the f/3.8 case. At 2 atm and 235 cm/s, the conversion efficiency first increased with power and then began to decrease, passing through a maximum of 33% near 500 W. In the third series, at 1.5 atm and 315 cm/s, there was no discernible trend in the total conversion efficiency, but this was the series in which the power absorption did not reach a peak, so the peak in conversion efficiency, if there is one, may occur at a higher power level than was reached. From these results, it appears that the effect of laser power level changes, at least in this range, is less important than the effects of pressure, focusing geometry, and flow speed.

Conclusion

It has been seen that, in contrast to earlier results, changes in incident flow rates, when the flow speeds are greater than those associated with buoyancy, have a significant effect on laser-sustained plasmas. Under conditions of low flow speeds, the LSP tends to propagate up the beam to the point of minimum maintenance intensity. High incident flow speeds can be used to force the plasma downstream into the region of maximum laser intensity, resulting in a significant improvement in the thermal conversion efficiency. In these experiments, the laser power was supplied by an annular beam. It is worth noting that the results of similar experiments with a Gaussian beam profile would likely be substantially different. The rate of change of the laser intensity on the axis would be smaller and there would be no possibility of an off-axis temperature peak. Under these conditions, much larger changes in the flow rate would likely be required in order to achieve changes in the plasma size and position similar to those observed with the annular beam. Significantly, the results of these experiments indicate that there are no "fatal flaws" in the concept of using the LSP for orbital transfer propulsion. It appears that it will be possible to tailor the LSP characteristics as necessary by varying the chamber pressure, flow patterns, and laser focusing geometry.

Acknowledgments

The authors gratefully acknowledge the contributions of Newton Wright, Fred Schwartz, and Jim White Jr. in the design, construction, and operation of the experimental apparatus. This work was supported by the U.S. Air Force Office of Scientific Research. The AFOSR Program Manager was Dr. Robert Vondra.

References

[1]Kantrowitz, A. R., "The Relevance of Space," *Astronautics and Aeronautics*, Vol. 9, Sept. 1971, pp. 34–35; also, "Propulsion to Orbit by Ground Based Laser," *Astronautics and Aeronautics*, Vol. 10, May 1972, p. 77.

[2]Myrabo, L. N., "Power-Beaming Technology for Laser Propulsion," *AIAA Progress in Astronautics and Aeronautics: Orbit-Raising and Maneuvering Propulsion: Research Status and Needs*, Vol. 89, edited by L. H. Caveny, AIAA, New York, 1984, pp. 3–29.

[3]Rosen, D. I., Pirri, H. H., Weiss, R. F., and Kemp, N. H., "Repetitively Pulsed Laser Propulsion: Needed Research," *AIAA Progress in Astronautics and Aeronautics: Orbit-Raising and Maneuvering Propulsion: Research Status and Needs*, Vol. 89, edited by L. H. Caveny, AIAA, New York, 1984, pp. 95–108.

[4]Glumb, R. J. and Krier, H., "Concept and Status of Laser-Supported Rocket Propulsion," *Journal of Spacecraft and Rockets*, Vol. 21, Jan.-Feb. 1984, pp. 70-79.

[5]McCay, T. D. and Dexter, C. E., "Chemical Kinetic Performance Losses for a Hydrogen Laser Thermal Thruster," AIAA Paper 85-0907, June 1985.

[6]Generalov, N. A., Ziniakov, V. P., Kozlov, G. I., Masyukov, V. A., and Raizer, Y. P., "Experimental Investigation of a Continuous Optical Discharge," *Soviet Physics—JETP*, Vol. 34, 1972, pp. 763-769.

[7]Klosterman, E. L. and Byron, S. R., "Measurement of Subsonic Laser Absorption Wave Propagation Characteristics at 10.6 Micrometers," *Journal of Applied Physics*, Vol. 45, 1974, pp. 4751-4759.

[8]Keefer, D. R., Henriksen, B. B., and Braerman, W. F., "Experimental Study of a Stationary Laser-Sustained Air Plasma," *Journal of Applied Physics*, Vol. 46, March 1975, pp. 1080-1083.

[9]Krier, H., Mazumder, J., Rockstroh, T. J., Bender, T. D., and Glumb, R. J., "Continuous Wave Laser Gas Heating by Sustained Plasmas in Flowing Argon," *AIAA Journal*, Vol. 24, Oct. 1986, pp. 1656-1662.

[10]Keefer, D. R., Crowder, H. L., and Peters, C. E., "Laser Sustained Argon Plasmas in a Forced Convection Flow," AIAA Paper 85-0388, Jan. 1985.

[11]Keefer, D. R., Welle, R. P., and Peters, C. E., "Power Absorption in Laser-Sustained Argon Plasmas," *AIAA Journal*, Vol. 24, Oct. 1986, pp. 1663-1669.

[12]Jeng, S. M., Keefer, D. R., Welle, R. P., and Peters, C. E., "Studies of Laser-Sustained Plasmas in Forced Argon Convective Flow, Part II: Comparison of Numerical Model with Experiment," *AIAA Journal*, to be published.

[13]Morris, J. C. and Yos, J. M., "Radiation Studies of Arc Heated Plasmas," ARL 71-0317, 1971.

[14]Kozlov, G. I., Kuznetsov, V. A., and Masyukov, V. A., "Radiative Losses by Argon Plasma and the Emissive Model of a Continuous Optical Discharge," *Soviet Physics—JETP*, Vol. 39, Sept. 1974, pp. 463-468.

[15]Kemp, N. H. and Lewis, P. F., "Laser-Heated Thruster Interim Report," NASA CR-161665 (PSI TR-205), Feb. 1980.

[16]Drellishak, K. S., Aeschliman, D. P., and Cambel, A. B., "Tables of Thermodynamic Properties of Argon, Nitrogen, and Oxygen Plasmas," AEDC-TR-64-12, 1964.

[17]Karzas, W. J. and Latter, R., "Electron Radiative Transitions in a Coulomb Field," *Astrophysical Journal, Supplement Series*, Supp. 55, Vol. VI, May 1961.

[18]Cheng, T. K. and Casperson, L. W., "Plasma Diagnosis by Laser Beam Scanning," *Journal of Applied Physics*, Vol. 46, May 1975, pp. 1961-1965.